Conference Proceedings of the Society for Experimental Mechanics Series

James De Clerck *Editor*

Topics in Modal Analysis I, Volume 7

Proceedings of the 32nd IMAC, A Conference and Exposition on Structural Dynamics, 2014

SEM

Springer

James De Clerck
Editor

Topics in Modal Analysis I, Volume 7

Proceedings of the 32nd IMAC, A Conference and Exposition on Structural Dynamics, 2014

Springer

Editor
James De Clerck
The Enterprise Program
Michigan Technological University
Houghton, MI, USA

ISSN 2191-5644 ISSN 2191-5652 (electronic)
ISBN 978-3-319-04752-2 ISBN 978-3-319-04753-9 (eBook)
DOI 10.1007/978-3-319-04753-9
Springer Cham Heidelberg New York Dordrecht London

Library of Congress Control Number: 2014931510

Printed on acid-free paper

Springer is part of Springer Science+Business Media (www.springer.com)

Preface

Topics in Modal Analysis I, Volume 7 represents one of the eight volumes of technical papers presented at the 32nd IMAC, A Conference and Exposition on Structural Dynamics, 2014, organized by the Society for Experimental Mechanics, and held in Orlando, Florida, February 3–6, 2014. The full proceedings also include volumes on Dynamics of Coupled Structures; Nonlinear Dynamics; Model Validation and Uncertainty Quantification; Dynamics of Civil Structures; Structural Health Monitoring; Special Topics in Structural Dynamics; and Topics in Modal Analysis II.

Each collection presents early findings from experimental and computational investigations on an important area within structural dynamics. *Topics in Modal Analysis I* represents papers on enabling technologies for modal analysis measurements such as sensors and instrumentation, and applications of modal analysis in specific application areas. Topics in this volume include:

Experimental techniques
Processing modal data
Rotating machinery
Acoustics
Adaptive structures
Biodynamics
Damping

The organizers would like to thank the authors, presenters, session organizers, and session chairs for their participation in this track.

Houghton, MS

J. De Clerck

Contents

Chapter 1
Infant Brain Response Against Shaking Vibration Using Finite Element Analysis

Takayuki Koizumi, Nobutaka Tsujiuchi, and Keisuke Hara

Abstract The most serious head injury resulting from shaken baby syndrome (infant brain injuries resulting from violent shaking attributed to child abuse) is acute subdural hematoma (ASDH). ASDH in infants has a high mortality rate and results in serious permanent injury. It is difficult gather accurate evidence from third parties since this abuse occurs mainly in the home mainly. As the result, medical practitioners rely on experience and intuition to determine the cause of infant head injuries. Therefore, in this study, we conducted simulation analysis that reproduced the shaking action—using a finite element model of an infant's head to provide a scientific basis for the determination of shaken baby syndrome. We used a model head of a 6-month-old that was constructed from adult head models and CT scan images of an infant head. The input value was defined as the angular velocity and head displacement obtained from the vibration experiments using a 6-month-old-infant dummy. ASDH is caused by the relative rotational motion between the skull and the brain with a rupture of the bridging veins that connect the skull and brain. Accordingly, we evaluated the relative movement between the skull and brain and measured the stretch ratio of the bridging veins. We then compared this ratio with the threshold, which is the rupture value. As a result, the violent shaking action regarded as shaken baby syndrome abuse results in ASHD when the bridging veins rupture. As the brain movement follows the skull, the bridging veins are stretched greatly depending on the forced skull movement and the brain's inertia.

Keywords Acute subdural hematoma (ASDH) • Finite element analysis • Shaken baby syndrome • Bridging veins rupture • Frequency

1.1 Introduction

Infant head trauma caused not by falling or other accidents, but by abuse such as dangerous shaking (shaken baby syndrome: SBS) has been reported [1]. Among severe cases of infant head trauma classified as SBS, acute subdural hematoma (ASDH) is prominent. The mortality rate due to ASDH is high and the survivors suffer substantial permanent damage. When assessing ASDH, it is difficult to obtain accurate testimony from third parties because such child abuse mainly occurs in the home. Therefore, a determination by medical authorities as to whether the injuries are the result of abuse or accident must be made based on experience and intuition, and thus lacks a scientific basis. Consequently, a means of clarifying the generating mechanism of ASDH in infants in necessary to provide a scientific basis for making such a judgment.

In this article, we perform experiments to evaluate the behavior of a dummy's head and what happens in the interior of the skull after vibration input to identify which vibration is a high risk for SBS injury. In the experiment, we used a 6-month-old dummy with a transparent skull head model and a vibration exciter to reproduce the shaking action. We also simulated the shaking action with a finite element model of a 6-month-old head. The finite element model was constructed using CT images and an existing adult head model. The input value is the displacement data and angle data obtained by the vibration experiments.

T. Koizumi • N. Tsujiuchi • K. Hara (✉)
Department of Mechanical Engineering, Doshisha University, 1-3 Tataramiyakodani, Kyotanabe-City, Kyoto 610-0321, Japan
e-mail: ksk.hara0511@gmail.com

J. De Clerck (ed.), *Topics in Modal Analysis I, Volume 7: Proceedings of the 32nd IMAC, A Conference and Exposition on Structural Dynamics, 2014*, Conference Proceedings of the Society for Experimental Mechanics Series,
DOI 10.1007/978-3-319-04753-9_1, © The Society for Experimental Mechanics, Inc. 2014

ASDH occurs as a result of relative rotational motion between the skull and the brain with a subsequent rupture of the bridging veins. Accordingly, we evaluated the stretch of the bridging vein model and relative rotational motion between the brain model and the skull model. We then evaluated the effect of the shaking vibration on the infant head and the resulting risk through comparative verification with the threshold, which resulted in a bridging vein rupture at a stretch ratio of 1.4 [2].

1.2 Threshold of Bridging-Vein-Rupture Stretch Ratio

Maw-Chang Lee et al. a performed tensile test using human bridging veins that were harvested from eight unembalmed cadavers aged 62–85 years. To evaluate bridging vein rupture, they used stretch ratio λ defined by the following equation:

$$\lambda = \frac{l}{l_0} \tag{1.1}$$

l_0 is the initial length of the bridging vein and l is the length during tensile strain.

Their reported maximum stretch ratio was approximately 1.5 at a strain rate of 200 s^{-1}. They also reported that the maximum value does not depend on the strain rate; the mean stretch ratio was 1.51 ± 0.24 and the mean load was 1.02 ± 0.92 N at a strain rate of 0.17 s^{-1}, and the mean stretch ratio was 1.55 ± 0.15 and the mean load was 0.99 ± 0.5 N at a strain rate of 170 s^{-1}.

In this study, we define the rupture value as 1.4, which is the minimum value at strain rate 170 s^{-1} because we assume the strain rate is higher during shaking.

1.3 Vibration Experiment Using 6-Month-Old Dummy

The shaking vibration produced by humans is not consistent. Therefore, we performed our experiments using a vibration exciter to set input parameters such as frequency and amplitude.

1.3.1 Six-Month-Old Anthropometric Test Dummy

We used a 6-month-old CRABI (client restraint/airbag interaction) dummy with a height of 67 cm and weight of 7.8 kg. This dummy has a transparent head model to visualize brain behavior in the skull. The x axis is aligned in the anterior posterior direction with positive x indicating the anterior direction. The y axis is aligned in the lateral direction, with positive y indicating the dummy's left side. The z axis is aligned in the superior–inferior direction, with positive z indicating the superior direction. Photographs of the dummy are shown in Fig. 1.1.

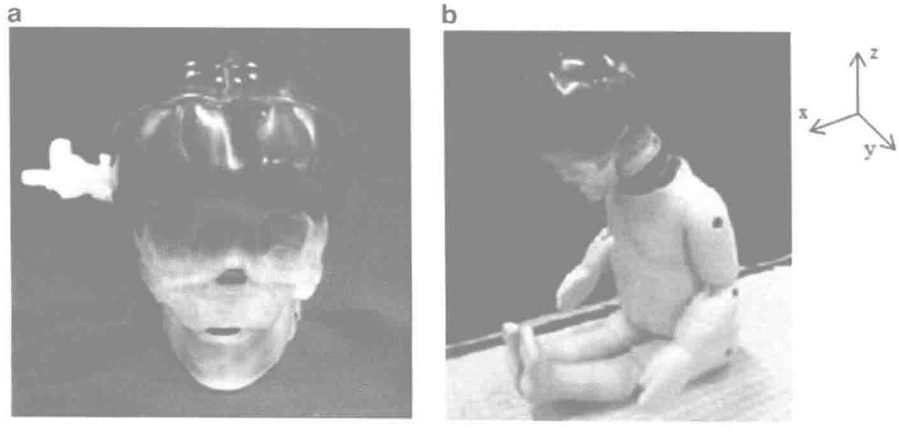

Fig. 1.1 CRABI 6 month-old. (**a**) Head model and (**b**) dummy

Fig. 1.2 Shaking experiment using vibration exciter

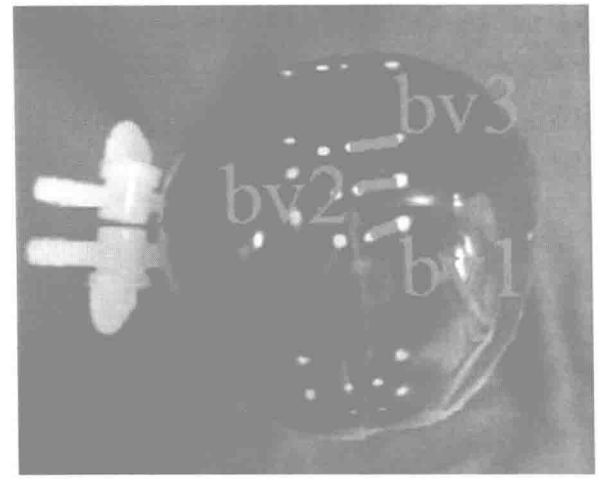

Fig. 1.3 Marker positions

1.3.2 Methods

The experiment model is shown in Fig. 1.2. The dummy was affixed on a board to transmit vibrations from the vibration exciter to the chest. We set up an angular velocity sensor and acceleration sensors to the dummy's head and attached an acceleration sensor to the chest. We then measured the acceleration and angular velocity. We applied white markers to the inner surface of the skull and the brain surface to measure the relative movement between the skull and brain. We set each combinations of brain and skull markers assumed to be the bridging veins as bv1–bv3. Figure 1.3 shows the marker combinations of brain and skull. Head behavior was taken at a sampling rate of 500 or 200 fps with two high-speed cameras (D-III: Detect). We then measured the relative displacement of the bv1–bv3 markers by converting the three-dimensional displacement method using the direct linear transformation (DLT) method. We calculated stretch ratio λ between two points as the evaluation strain parameters of the bridging veins. We used Eq. (1.1) to calculate the ratio, using distance l_0 of the bv1–bv3 in the video frame and distance l of bv1–bv3 in the initial position. We then evaluated the relative displacement between the brain and the skull.

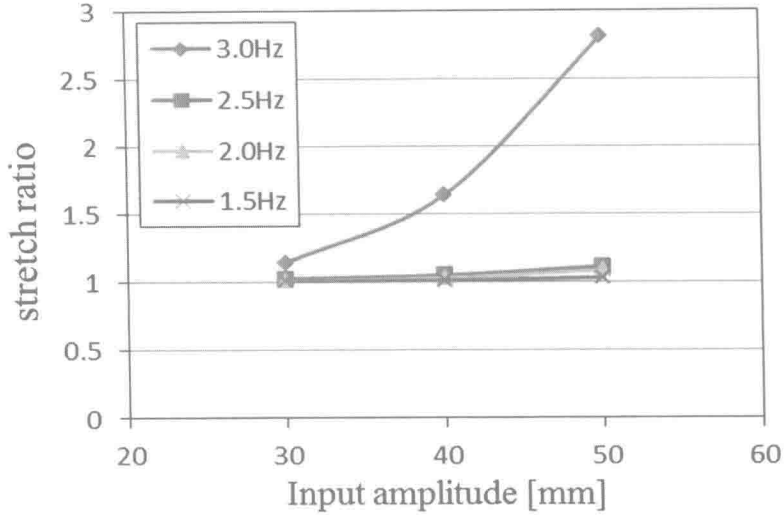

Fig. 1.4 Maximum stretch ratio responses via high-speed camera images

1.3.3 Input Vibration

We performed experiments for only the x axial, which is the main component of the shaking vibration. In addition, we ignored vertical vibration in error of less than 5 % compared with the two-axis coupled vibration. The input values were a total of 12 patterns, combining three amplitude patterns (±30.0, ±40.0, and ±50.0 mm) in the x axial with four frequency patterns (1.5, 2.0, 2.5, and 3.0 Hz). To reproduce the human act of shaking an infant, the input amplitudes were set to the value close to the one at which people shook the infant dummy. In addition, the input frequencies were set at a lower value than the maximum high-risk frequency (around 3.0 Hz) obtained by a previous study. In the previous study, the dummy's head, which was a rigid model, was swung most at the 3.0-Hz frequency.

1.3.4 Results and Discussion

Our results are reported in Fig. 1.4 in terms of the maximum bridging-vein stretch ratio and the amplitudes for each condition. The maximum of the bridging-vein stretch ratio tends to increase with increasing amplitude at any frequency, as shown in Fig. 1.4. Therefore, the breaking risk for the bridging veins becomes higher as amplitude increases. For a ±40 mm or more amplitude at the 3.0-Hz frequency, the stretch ratio between two points shows as large value and is significantly higher for ±50.0 mm amplitude. Therefore, there is a possibility that the bridging veins will rupture at this vibration. On the other hand, the value shows a small shift at any amplitude of 2.5 Hz and under. In other words, the bridging veins do not break at 2.5 Hz or under. Therefore, we can conclude that ASDH due to rupture of the bridging veins does not occur with vibrations caused during cradling.

1.4 Simulation Analysis Using 6-Month-Old Finite Element Model

We performed finite element analysis of shaking action using with the 6-month-old head model using the same method as in the experiments. We used PAM-CRASH (ESI Group) as the dynamic explicit analysis solver.

1.4.1 Original Finite Element Model of 6-Month-Old Head

A highly accurate infant head model cannot be constructed because the characteristics of skull shape are different for infants and adults. Therefore, scaling down an adult head model to a finite element model of the infant head is not appropriate. In this study, we used the finite element model of a newly constructed 6-month-old head based on three-dimensional shape

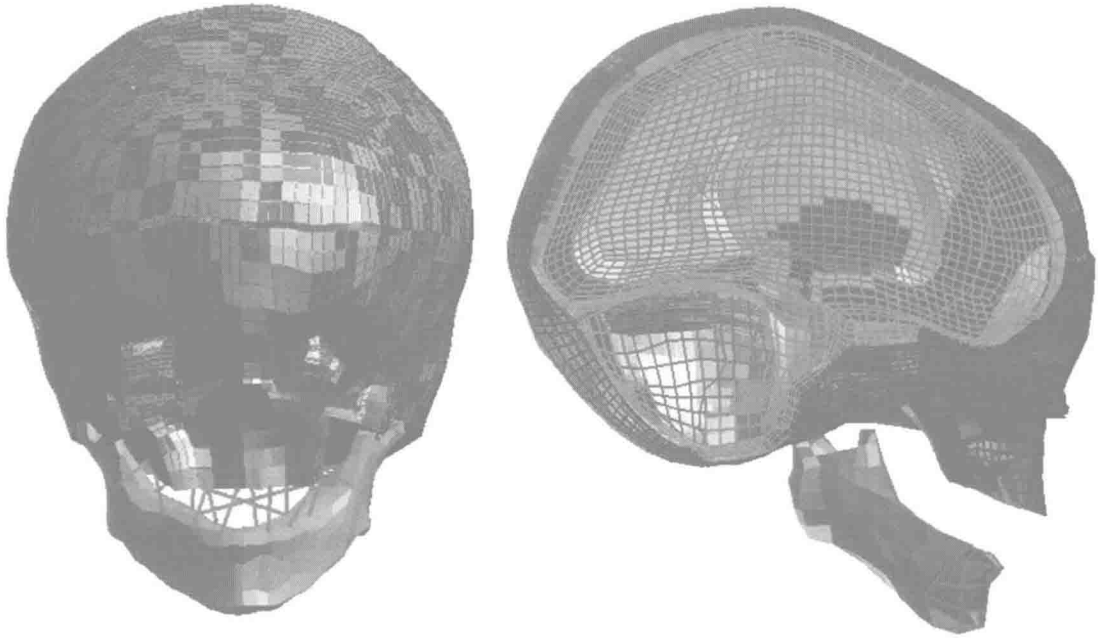

Fig. 1.5 Finite element original model of 6-month-old head

Table 1.1 Dimension of 6-month-old head (mm)

Length	Breadth	Height
154.9	119.4	147.3

data of the head obtained from CT images of a particular 4-month-old head. The shape of the finite element model of an adult head was then converted into the 4-month-old head model based on the shape data using the free-form deformation transformation (FFD) method. The 6-month-old infant head finite element model was constructed by scaling the dimensions of the 4-month-old head that had been converted to the shape of the 6 month-old CRABI head. The original head model is composed of a skull including structure and anterior fontanel, cerebrospinal fluid (CSF), brain (left and right cerebrum, cerebellum, and brainstem), membrane (dura mater, pia mater, flax, and tentorium), and bridging veins. The total number of nodes is 121.561 and the total number of elements is 151.720. Figure 1.5 illustrates the original model and Table 1.1 shows the main dimensions.

1.4.2 Reducing Original Finite Element Model of 6-Month-Old Head

The original model required a substantial amount of computation time, as each node has 6° of freedom. Therefore, in this study, we reduced the original finite element model of the 6-month-old head without changing the shape of the skull model, brain model, and bridging model, which are important objects. The adult skull has three layers, an inner table, outer table, and skull dipole, and the structure and anterior fontanel are closed for completing ossification. On the other hand, the infant skull has a single layer without an inner and outer table, and the structure and anterior fontanel exist because of incomplete ossification. In addition, the skull model is regarded as a rigid body for high strength and high density compared to the inside of the skull. On this basis, we simplified the skull and structure as Shell elements and defined their rigid bodies. Moreover, the original model has microelements of a partially asymmetrical and complicated shape. This analysis tool, which decides the time step for the distance of nodes, requires a substantial amount of computation time. Therefore, we re-built each part symmetrically centered at the X–Z plane. We also united the left and right cerebrum, cerebellum, and brainstem as a brain group having the same material properties. The CSF was constructed as a smoothed particle hydrodynamics (SPH) model,

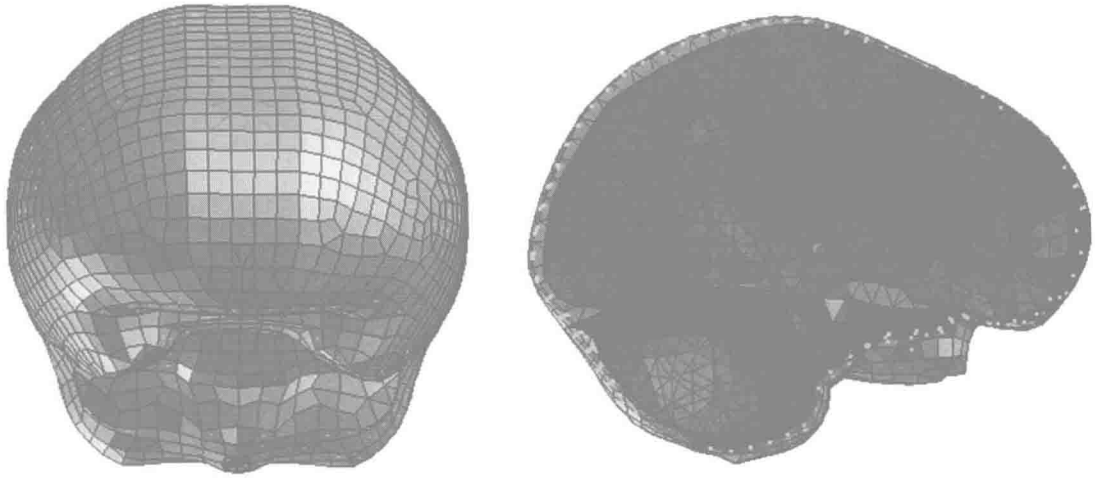

Fig. 1.6 Finite element model of the 6-month-old infant head

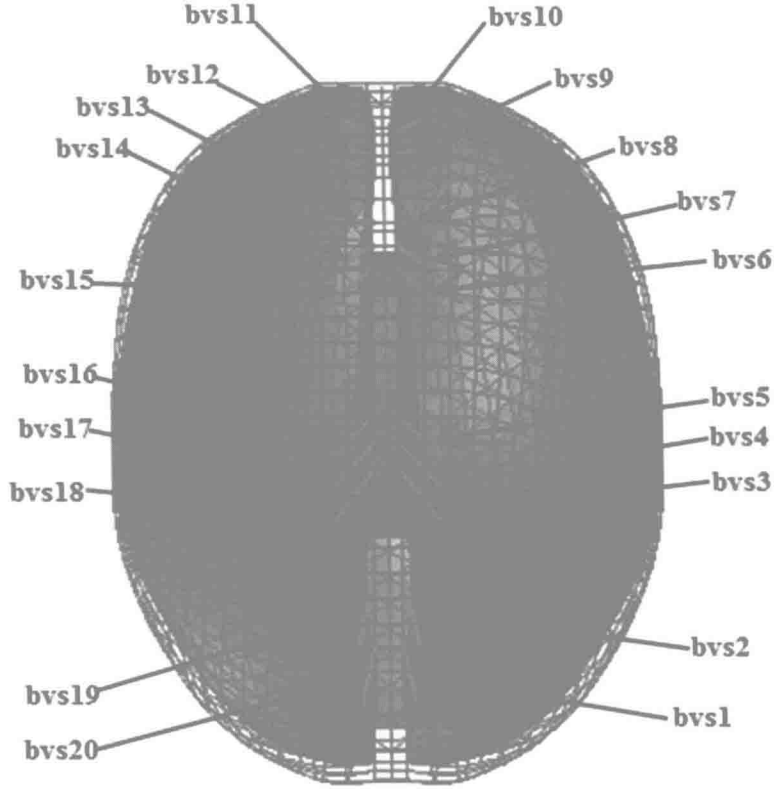

Fig. 1.7 Bridging veins of the finite element model

which enables calculation of large deformation for the continuum analysis method of a compressible fluid model. The bridging veins were constructed 20 models connecting the pia matter and dura matter at the sagittal plane where ASDH is likely to occur. We consulted Zhou et al. [3] and Oka et al. [4] to obtain their connecting location and angle. Figure 1.6 shows our finite element 6-month-old head model. Figure 1.7 shows the bridging veins (bvs1–bvs20). The model is composed of a rigid skull, CSF, the brain group, membrane (dura mater, pia mater, flax, and tentorium), and bridging veins. The brain group model is Solid, the rigid skull model and membrane models are Shell, the CSF model is SPH, and the bridging vein model is Beam. The total number of nodes is 10,516 and the total number of elements is 27,872.

Table 1.2 Material properties (1)

Part	Material property	Density, ρ (kg/m^3)	Young's modulus, E (GPa)	Poisson's ratio, ν
Brain group	Linear viscoelastic	1,040	K = 2.19	
Pia mater	Elastic	1,133	1.15×10^{-2}	0.45
Dura mater		1,133	3.15×10^{-2}	0.45
Falx		1,133	3.15×10^{-2}	0.45
Tentorium		1,133	3.15×10^{-2}	0.45
Sagittal sinus		1,133	3.15×10^{-2}	0.45
CSF	SPH	1,060	K = 2.19	
Structure	Elastic	2,150	4.2×10^{-3}	0.22
Inner table	Elastic	2,723	15	0.21
Bridging vein	Elastic	1,133	9.43×10^{-3}	0.45

Table 1.3 Material properties (2)

Part	Density (kg/m^3)	Bulk modulus (GPa)	Short time shear modulus (GPa)	Long time shear modulus (GPa)	Decay constant (s^{-1})
Brain	1,040	2.19	$2{,}710 \times 10^{-9}$	891×10^{-9}	166

1.4.3 Material Property

The brain group is a viscoelastic model and the deviation response is a dominated Zener model, which is a parallel model using a Maxwell model and a spring model. This shear stress-relaxation behavior, response against step function, is defined by the following equation.

$$G(t) = G_\infty + (G_0 - G_\infty)\, e^{-\beta t} \tag{1.2}$$

G is the relaxation modulus, G_0 is the instantaneous modulus, G_∞ is the equilibrium modulus, β is the decay constant, and t is the duration. Each value was obtained from Fallenstein et al. [5]. The CSF viscous fluid was reproduced using the Monaghan-Gingold method [6] and the material property was water because CSF is very similar to water. The bridging vein model is defined as an elastic body and the material property is obtained from the experiment performed by Lee et al. [2]. They publish bridging veins rupture when the mean strain is 0.5 and the load is 1.0 N. The bridging veins dimension is reported mean length 6.2 mm, mean circumference 4.4 mm, mean thickness 0.05 mm. We calculated Young's modulus (E) 9.43 MPa from these values. And other properties are given the same characteristics as the adult [7–9]. The average head mass of 6-month-old is 2.3 kg. Therefore, we added mass to each part comparing to original model to be the 2.3 kg. Tables 1.2 and 1.3 show the material property of each part.

1.4.4 Simulation of Shaking Vibration

To simulate shaking by a human, we verified the effect of the presence or absence of bridging veins and only rotational motion or only translational motion. The input value was the displacement data and angle data obtained from the vibration experiments. For comparison, we used the experiment data of the ±50 mm chest amplitude and 3 Hz, which showed the maximum bridging-vein stretch ratio. As we reproduced the exact behavior due to forced displacement, we reduced the noise of the measured experimental data with a low-pass filter. We then calculated the integral to get the displacement data and the angle data. Figure 1.8 shows the displacement data and angle data as the input data. In Fig. 1.8, the input data can be regarded as reasonable because the dummy's head behavior showed approximately ±130 mm amplitude at 3 Hz in the experiment.

At the start of the simulation, we performed comparative verification of the head behavior between the experiment and the simulation. We extracted the dummy's head trajectory at one cycle every 1/30 s, at which the behavior was stable. Figure 1.9 shows the head trajectory of the experiment. Next, we performed simulation of shaking vibration by setting the input data to the center of gravity. Figure 1.10 shows the input position. We then extracted the head trajectory at one cycle at the same time as in the experiment. Figure 1.11 shows the head trajectory of the simulation. These two trajectories are almost identical.

Second, we calculated the stretch ratio of the bridging vein model using Eq. (1.1).

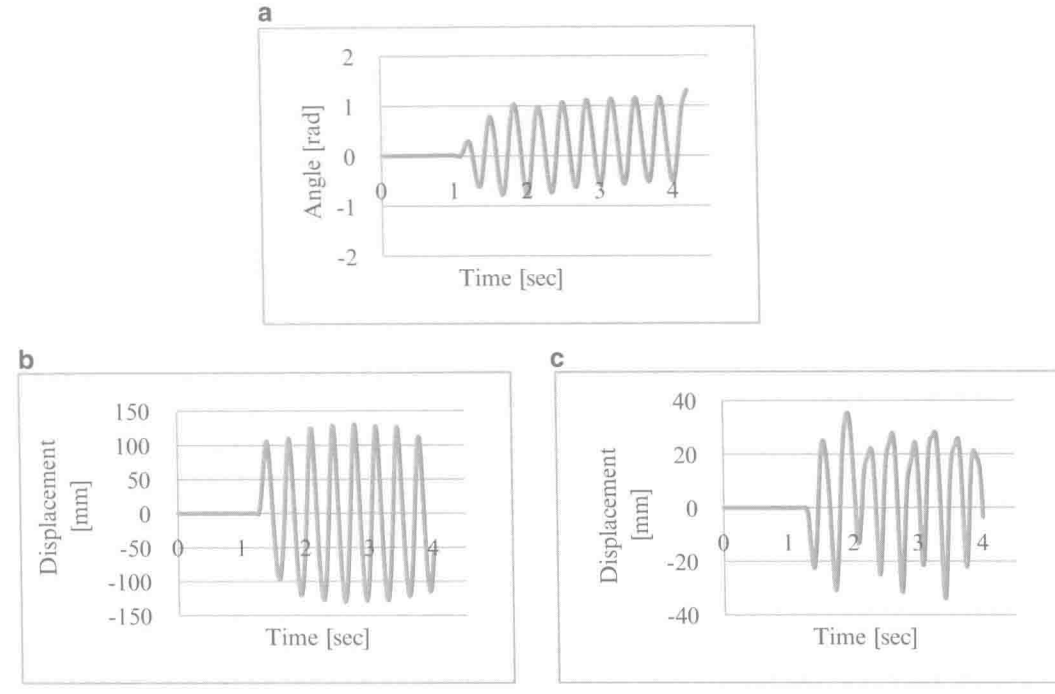

Fig. 1.8 Input condition of analysis. (**a**) Angular data, (**b**) displacement data (X axis), and (**c**) displacement data (Z axis)

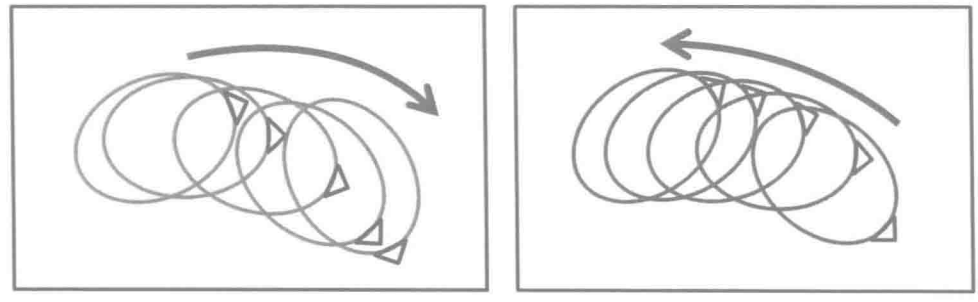

Fig. 1.9 Head trajectory of experiment. (**a**) Toward the front from the back (1/30–5/30 s) and (**b**) front to back (6/30–10/30 s)

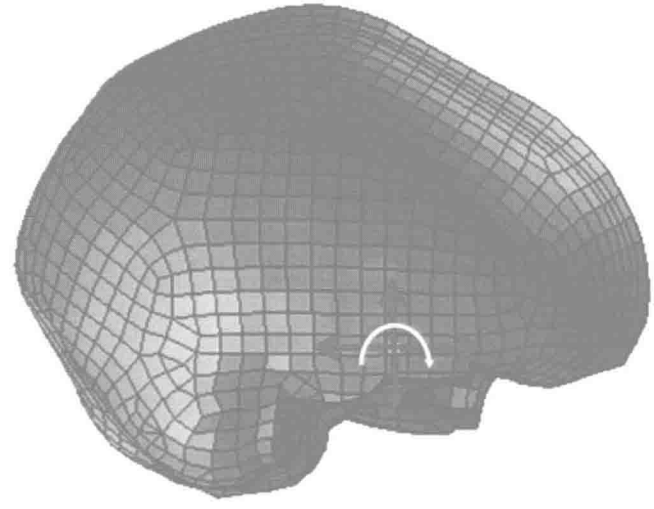

Fig. 1.10 Shaking simulation condition

Fig. 1.11 Head trajectory of simulation. (**a**) Toward the front from the back (1/30–5/30 s) and (**b**) front to back (6/30–10/30 s)

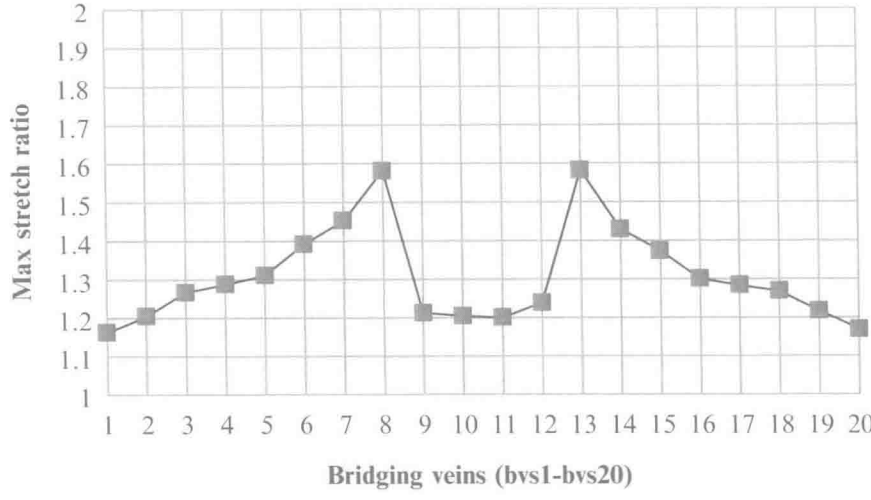

Fig. 1.12 Maximum bridging-vein stretch ratio

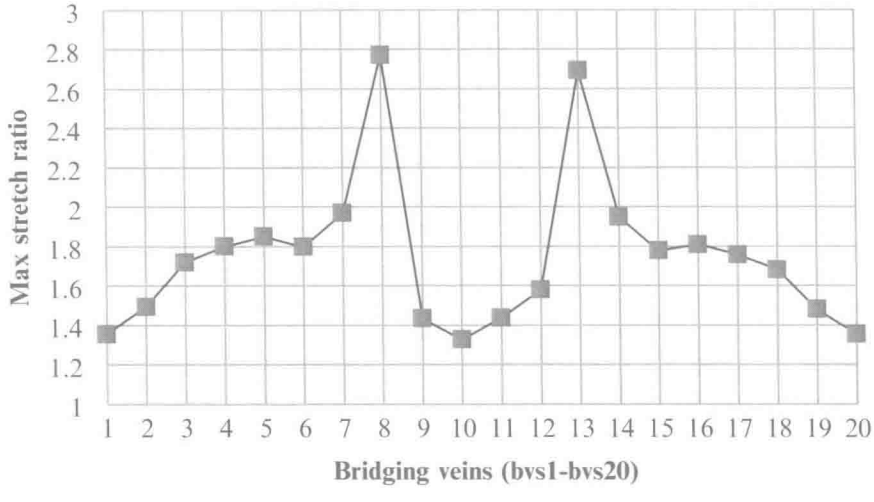

Fig. 1.13 Maximum assumed bridging-vein stretch ratio

1.4.5 Result of Simulation

Figure 1.12 shows the maximum stretch ratio of bvs1–bvs20. In the model without bridging veins, we measured the distance between the nodes assumed to be bridging veins during the simulation. Figure 1.13 shows their maximum stretch ratio. In Fig. 1.13, the peak value is 2.77 for bvs8. In the experiment, the maximum value was 2.8 at the ±50 mm amplitude and 3 Hz frequency. Therefore, the model is valid. In Fig. 1.12, the peak value is 1.58 of bvs13 over a threshold of 1.4 [2]. Therefore, this represents the violent shaking action regarded as child abuse in which ASDH with the bridging vein rupture occurs.

Moreover, we verified the effect of rotation and translation. Figures 1.14 and 1.15 show the maximum stretch ratio of rotation and translation. The peak value is 1.30 for bvs14 for rotation and 1.54 for bvs8 for translation. For the bridging vein's stretch, the translation movement has larger brain behavior than rotation. We believe this is caused by the occipital area's space.

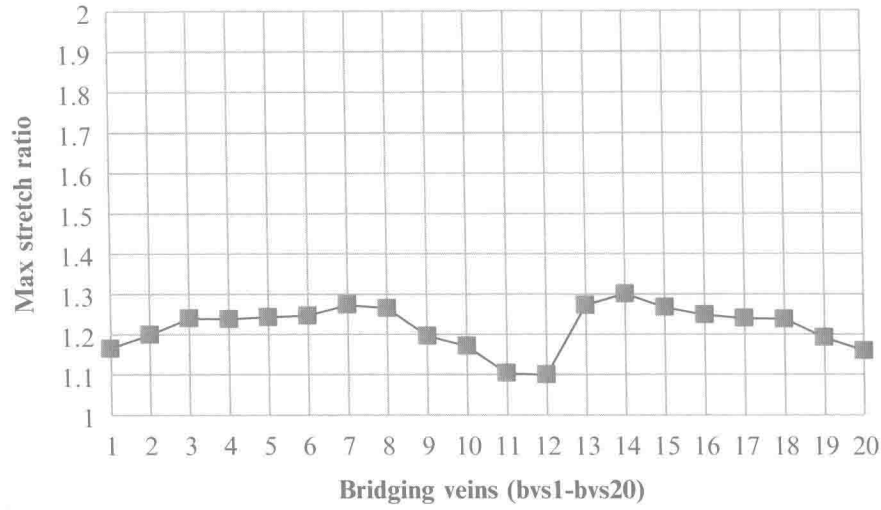

Fig. 1.14 Maximum bridging-vein stretch ratio (rotation)

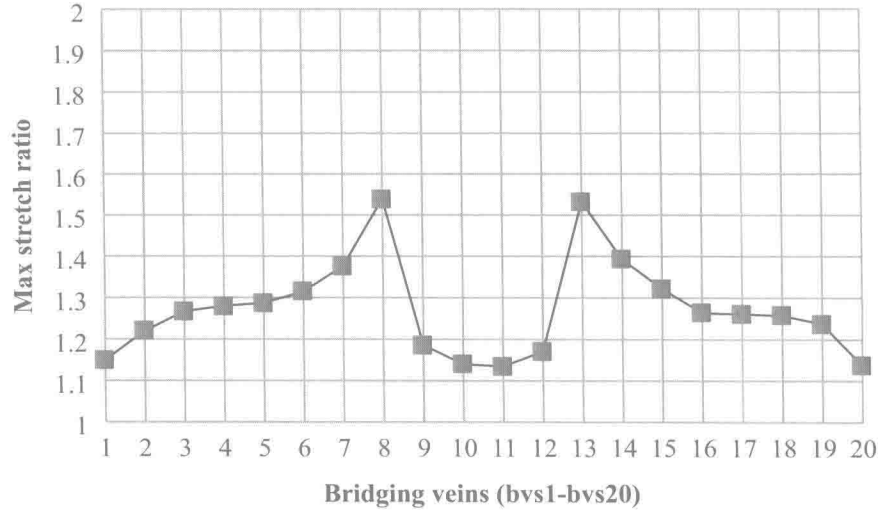

Fig. 1.15 Maximum bridging-vein stretch ratio (translation)

The maximum tension in shaking occurs at the frontal region when the head moves toward the front form the back. This area is relatively consistent with the area where ASDH is likely to occur. The maximum tension occurs when the skull is forced front and the brain's inertia as a result because the brain behavior follows the skull's movement. Therefore, we found that bridging veins rupture due to brain's phase lag against the skull and the possibility of rupture is lower with relative rotational movement due to a difference in vibration frequency.

1.5 Conclusion

1. In the experiment, ASDH is likely to occur for severe vibration such as the frequency is 3.0 Hz and the amplitude is 50.0 mm.
2. In finite element analysis, the model is reasonable since similar results with experiment.
3. For bridging veins stretch, the violent shaking action occur bridging veins rupture and ASDH.
4. As brain move in a phase lag against skull, bridging veins are stretched greatly depending on the skull forced front and the brain's inertia.

Acknowledgments This work was partially supported by Grant-in-Aid for Scientific Research (C) (23560272), Japan Society for the Promotion of Science. And also, this was supported by Associate Professor Yusuke Miyazaki at Tokyo Institute of Technology for 6-month-old dummy and original simulation model. Express our gratitude to write.